International Journal of Science and Research (IJSR)
ISSN: 2319-7064
ResearchGate Impact Factor (2018): 0.28 | SJIF (2018): 7.426

# Adsorption of Eriochrome Black T (EBT) Onto Activated Carbons Obtained from *Cola Anomala* Nut Shells by Chemical Activation with Phosphoric Acid ($H_3PO_4$)

**Jacques Bomiko MBOUOMBOUO[1], Caroline Lincold Nintedem Magapgie[2], Charles Melea Kede[3], Harlette Poumve Zapenaha[4], Pierre Gerard Tchieta[5*]**

Chemistry Laboratory, Faculty of Science, University of Douala; BP 24157 Douala, Cameroon
Corresponding Author: Pierre Gerard TCHIETA *
E-mail: pgtchieta[at]yahoo.fr

**Abstract:** ***The objective of this work is to prepare an active carbon with the best adsorption properties from the shells of Cola nuts (anomala) for the reduction of Eriochrome Black T in aqueous medium. The materials (shells nut of Cola anomala) obtained were characterized by Thermogravimetric Analysis (TGA), $pH_{PCN}$ and Fourier Transform Infrared (FT-IR). The study of adsorption involves discussing the effects of contact time and initial solute concentration using a batch adsorption technique. The effect of temperature made it possible to carry out a thermodynamic study to define the nature of the adsorption phenomena. In addition, different kinetic models (first and second order and Intra-particle) and adsorption isotherms (Langmuir and Freundlich) were used for the evaluation of the adsorption capacity. The TGA analysis illustrates the presence of: hemicellulose, cellulose and lignin thus confirming the lignocellulosic structure of the activated carbon obtained. The CA1/2 and CA1/3 samples prove to be the best absorbers. The measurement of their zero charge point pH gives respectively $pH_{PCN}$ = 6.8 and $pH_{PCN}$ = 6.9, showing the almost neutral character of the surface of these active carbons. The kinetic model of the pseudo-second order better describes the adsorption of EBT on AC with $R^2 \geq$ 0.99950. The thermodynamic study gave the negative values of the free energy justifying the spontaneous nature of the process and which thus shows that the adsorption is of physical type. The process is endothermic with respect to the positive values of free enthalpy obtained. Positive values of entropy justify the good affinity of the EBT on the AC due to the swelling of the pores.***

**Keywords:** Activated carbon, Kinetic, Thermodynamic, Adsorption, Synthetic dye

## 1. Introduction

Water is the major constituent of our planet. This substance is of great interest for humans in their multiple needs and for the balance of aquatic ecosystems. But, it is unfortunately very easy to pollute by industrial, agricultural, domestic activities as well as by urban waste including many toxic substances which cause a degradation of its physical, chemical or biological properties [1].

Eriochrome Black T (EBT) is an azo sulphonic dye belonging to the class of anionic acid dyes, widely used in textile industries because of its dyeing form [2]. Adsorption is highly recommended for the elimination of organic and inorganic pollutants at low concentrations. It requires a microporous adsorbent, capable of exchanging ions and creating chemical bonds [3-6]. There are a wide range of adsorbent materials such as silica gel, zeolites, synthetic adsorbents (resins), clays, activated alumina, industrial wastes, bioadsorbents and activated carbon [3,4,6,7, 8,9,10].

Activated carbon is cited preferentially among the many materials considered as the most promising for the removal of organic and inorganic micropollutants [11]. Various studies have been devoted to the production of activated carbons from lignocellulosic residues: pecan nuts [11], almond [12], coconut [13-14], date kernels [15], cores of other fruits [16-18], woods [19], cloves of Flamboyant Delonixregia [20].

Activated carbon is obtained either by chemical activation or by physical activation. Among the chemical activators, phosphoric acid and zinc chloride are the most used [11, 15, 21, 22]. But some bases such as KOH [23-24], NaOH [23, 25, 26], $K_2CO_3$ [27], $Na_2CO_3$ [26] are also used as chemical activators. Some researchers have reported that the propensity of the chemical activation method to $H_3PO_4$ and $ZnCl_2$ is related to its low activation temperature (400-500 °C) compared to physical activation (temperature above 850 °C), shorter processing times and better quality of activated carbons obtained [11, 28, 29]. Specifically, chemical activation with $H_3PO_4$ gives activated carbons with improved efficiency for the removal of organic and inorganic micropollutants due to better porosity development, specific surface areas and pore volume [22, 28].

The objective of this work is to prepare an active carbon with the best adsorption properties from the shells of *Cola* nuts (*anomala)* for the reduction of Eriochrome Black T in aqueous medium.

The work consisted of preparing active carbon from *Cola anomala* nut shells by chemical activation with phosphoric acid ($H_3PO_4$). Activated carbons were characterized and tested for the adsorption of Eriochrome Black T (EBT) in an aqueous medium. The study of adsorption consisted of discussing the effects of contact time and initial solute concentration using a batch adsorption technique. The effect of temperature made it possible to carry out a

thermodynamic study to define the nature of the adsorption phenomena. In addition, different models of kinetics (first and second order and Intra-particle) and adsorption isotherms (Langmuir and Freundlich) were used for the evaluation of the adsorption capacity.

## 2. Experimental

### 2.1 Preparation of activated carbon

The shells of *Cola anomala* nuts of the Malvaceae family were harvested in the outskirts of Foumban (Koupa Ngagnou) located 7 km away in the Noun region of western Cameroon. After collection, pods of Cola anomala nuts were thoroughly washed with tap water and rinsed with distilled water to remove impurities and then dried in the sun for 15 days. In addition, they were milled using a mill-type grinder coat and then sieved through two sieves RETSCHAS200 type to retain only particles with a particle size of between 32 and 63 $\mu$m. Thus, the powder retained is pretreated chemically before carbonization. The experimental protocol is taken from [30].

The technique consists of mixing in a beaker, a determined mass of sieved powder with the phosphoric acid oxidant in a weight ratio 1/1, 1/2 and 1/3. The mixture was stirred mechanically for 2 hours of contact time. The samples were then incubated at 110 °C. for 24 h and then cooled to await carbonization (pyrolysis). The impregnate was placed in the NABERTHERM brand calcining furnace (30-3000 °C) in a ceramic crucible at a maximum temperature of 450 °C with a rise rate of 5 °C/min and an hour of stay. Any residues of carbonization are removed by an abundant washing with distilled water until neutralization of the rinsing water by regular checking of the pH = 7. Before carrying out the adsorption tests, the activated carbon is dried in an oven at 110 °C for 24 hours.

### 2.2 Characterization of powder and prepared activated carbon

The lignocellulosic constituents and the maximum carbonization temperature of the sieved powder of the *Cola anomala* nut shells were determined by thermogravimetric, differential thermal analysis and differential scanning calorimetry (TG-DTG-DSC). The chemical functions present on the surface of the precursor material and the prepared activated carbon are determined by the Fourier transform infrared (FTIR). The sampling method consists of obtaining pellets by compression of the samples with potassium bromide (KBr). The samples were made by scanning the wave numbers from 4000 to 400 $cm^{-1}$ using an FTIR spectrometer.

### 2.3 pH at zero charge point ($pH_{PCN}$)

The experimental protocol used is that of Lopez (1999) [31]. For this purpose, a volume of 30 ml of a solution of sodium chloride (NaCl) 0.1 M was contacted with a mass of 0.1 g of activated carbon for 8 hours. The measured pH values were: 2, 4, 6, 8 and 10. They were adjusted by addition of 0.1 M HCl or NaOH using a Hanna pH meter.

### 2.4 Iodine number

The samples studied were characterized by measuring the iodine number (mg/g) using an iodine solution of 0.02 N. A volume of 40 ml of the iodine solution was treated with mass of 0.1 g of activated carbon for 4 min. After equilibrium, 10 ml of the iodine filtrate was titrated with 0.1 N sodium thiosulfate in the presence of a colored indicator. The iodine value $I_2$ (mg/g) can be calculated by the following formula:

$$Q_e = I_2 = \frac{(V_B - V_S)}{m} \times N \times (126{,}9) \times \frac{40}{10} \quad (1)$$

Where: $(V_B\text{-}V_S)$ is the difference between the results of the titration to the white test and to the test with adsorbent in ml of 0.1 N $Na_2SO_4$, N is the normality of the solution $Na_2SO_4$ in mol/L, 126.9 is the atomic mass of iodine (g/mol) and m is the mass of the adsorbent (g).

The knowledge of the quantity of iodine adsorbed at equilibrium per gram of activated carbon ($Q_e$) leads to the determination of the specific surface ($S_{I2}$) by the application of the relation:

$$S_{I2} = Q_e \sigma N_A / MI_2 \ (m^2.g^{-1}) = 1{,}28.10^5 \ Q_e / MI_2 \ (m^2.g^{-1}) \quad (2)$$

The area occupied by an iodine molecule is equal to σ = 21,3 $Å^2$ et $N_A$ = 6,023.$10^{23}$ is the Avogadro number and the molar mass of iodine (MI2) is 126.9.

### 2.5 Methylene blue number

A volume of 50 ml of a methylene blue solution of a concentration of 25 mg/L was treated with a mass of 0.05 g of activated carbon for 2 hours. The filtrate was measured out to the UV-visible spectrophotometer of mark SCHOTT Instrument to a wavelength of 659 nm. The removal rate (Rd%) and the adsorbed amount (Qe, mg/g) of methylene blue are determined by the following formulas:

$$Rd\,(\%) = \frac{C_0 - C_e}{C_0} \times 100 \quad (3)$$

$$Qe = \frac{C_0 - C_e}{m} \text{ x } V \quad (4)$$

Where: $C_o$ is the Initial Concentration of MB (mg/L), $C_e$ is the Concentration of MB in the equilibrium mixture (mg/L), m is the mass of the adsorbent (g) and V is the Volume of the solution containing the MB (ml).

The $S_{MB}$ specific surface area determined using MB is estimated by the following equation:

$$S_{MB} = Q_e . A_m . N_A / M_{MB} \quad (5)$$

With: $S_{MB}$ is the specific surface area determined using MB as adsorbate ($m^2/g$); (Am) is the air occupied by a molecular of MB (175 $Å^2$), $Q_e$ is the adsorption capacity of MB (mg/g), $N_A$ is the number of Avogadro (6,023.$10^{23}$ $mol^{-1}$) and MB is the MB molar mass of (319.85 $g.mol^{-1}$) [32].

### 2.6 Ash rate

An initial mass of 0.5 g of activated carbon ($M_1$) was calcined in an oven at a maximum temperature of 700 ° C with a heating rate of 5 ° C/min and 5 minutes of residence.

Finally, we weigh again the initial mass of the activated carbon after calcination is ($M_2$).

The ash rate is given by the following equation:

$$\%C = \frac{M_2}{M_1} \times 100 \quad (6)$$

### 2.7 Eriochrome Black T (EBT) adsorption study on prepared activated carbon

The experiments are executed in batch mode regardless of the parameter studied. To this end, we introduced a mass of activated carbon into an Erlenmeyer flask and a volume of 30 ml of a solution of Eriochrome Black T (EBT) of desired concentration. Then, the mixture was stirred magnetically at room temperature for a definite time. After stirring, the mixture was filtered using Whatman type filter paper and the filtrate was measured out to the UV-visible spectrophotometer (320-800 nm) of mark SCHOTT Instrument to a maximum wavelength (λmax = 572 nm).

#### 2.7.1. Studies of kinetic models

The following three mathematical models were tested to model the kinetic adsorption of activated carbon Eriochrome Black T:

##### 2.7.1.1. Kinetic pseudo-first order model (Lagergren, 1898)

The linear form of the pseudo-first order model is given by the following relation:

$$\mathrm{Ln}\,(Q_e - Q_t) = \mathrm{Ln}\,Q_e - K_1 t \quad (7)$$

With: $k_1$ the rate constant for kinetic of the pseudo first order, $Q_t$ and $Q_e$ the adsorption capacities at time t [mg of adsorbate/g of adsorbent] and at equilibrium [mg of adsorbate/ adsorbent], respectively. The constants of the model are determined graphically by plotting Ln $(Q_e - Q_t)$ against t. In addition, the equilibrium half-adsorption time ($t_{1/2}$, min) and the difference between the equilibrium adsorption capacities $(\Delta q)$ are determined by the following equations:

$$t_{1/2} = \frac{Ln2}{K_1} = \frac{0{,}693}{K_1} \quad (8)$$

$$\Delta q = \left| Q_{emax}\,(\exp) - Q_e\,(\mathrm{th}) \right| \quad (9)$$

Where: $Q_{emax}$ (exp) is the adsorption capacity obtained experimentally and $Q_e$ (th) is the theoretical adsorption capacity deduced from the kinetic relationships.

##### 2.7.1.2. Kinetic pseudo-second order model

The linear form of the pseudo-second order model is given by the following equation:

$$\frac{t}{Q_t} = \frac{1}{K_2 Q_e^2} + \frac{1}{Q_e}\, t \quad (10)$$

Where: $k_2$ is the constant for second-order kinetic (g.m$g^{-1}.min^{-1}$), $Q_t$ and $Q_e$: adsorption capacities at time t [mg of adsorbate/g of adsorbent]] and at equilibrium [ mg of adsorbate/g of adsorbent], respectively. The adsorption kinetic constant $K_2$ and the quantity of solute adsorbed at equilibrium $Q_e$ are determined experimentally from the plot of t/Qe = f (t). Thus, the half-adsorption time (t1/2) in ($min^{-1}$), the difference ($\Delta q$) and the initial adsorption (h) in (mg.$g^{-1}min^{-1}$) are obtained from the following relationships:

$$t_{1/2} = \frac{1}{K_2 Q_e\,(th)} \quad (11)$$

$$\Delta q = \left| Q_{emax}\,(\exp) - Q_e\,(\mathrm{th}) \right| \quad (12)$$

$$h = K_2.Q_e^2\,(\mathrm{th}) \quad (13)$$

Where: $Q_{emax}$ (exp) is the adsorption capacity obtained experimentally.

##### 2.7.1.3. Kinetic model of intra-particle diffusion

The linear model of intra-particle scattering is described by the following equation:

$$Q_t = K_d \times t^{1/2} + I \quad (14)$$

Where: $K_d$ is the intra-particle diffusion constant (mg.$g^{-1}.min^{-1/2}$) and I is the boundary layer thickness constant (mg/g).

The representation of $Q_t$ as a function of ($t^{1/2}$) makes it possible to calculate $K_d$, I and to highlight the various stages of the adsorption process.

### 7.2. Isothermal models

The binding data of Eriochrome Black T on activated carbon are processed according to the linear **Langmuir** and **Freundlich** equations.

The linear form of the Langmuir isotherm is given by the following equation:

$$\frac{1}{Q_e} = \frac{1}{K_L\, Q_{max}\, C_e} + \frac{1}{Q_{max}} \quad (15)$$

Where: $C_e$ is the EBT concentration at equilibrium (mg/L), $Q_e$ is the amount of the adsorbed NET per unit mass of adsorbent (mg/g), $Q_{max}$ is the theoretical maximum adsorption capacity (mg/g) g) and $K_L$ is the Langmuir constant of the adsorption equilibrium (L/mg).

The lines are obtained from the plot of $\frac{1}{Q_e}$ = f ($\frac{1}{C_e}$).

The linear form of the Freundlich isotherm is given by the following expression:

$$\mathrm{Log}(Q_e) = \log\,(K_F) + \frac{1}{n_f} \log\,(C_e) \quad (16)$$

Where: nf is the constant indicative of the adsorption intensity, $C_e$ is the EBT concentration at equilibrium (mg/L) and $K_F$ is the constant relative to the adsorption capacity of the adsorbent (Freundlich constant ) ($mg^{1-(\frac{1}{n})}.L^{1/n}.g^{-1}$). The parameters $K_F$ and $n_F$ are determined from the graphical representation of Log ($Q_e$) = f (log ($C_e$).

## 3. Results and Discussion

### 3.1 Characterization of powder and activated carbons prepared from *Cola anomala* nut shells

#### 3.1.1. Thermogravimetric analysis

Figure 1 shows the thermogram coupled to TG/DTG/DSC.

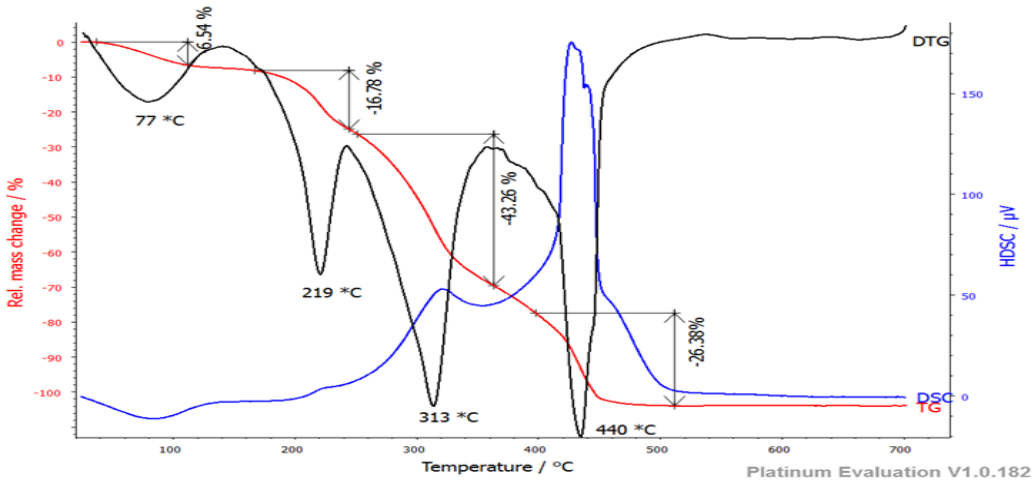


**Figure 1**: Coupled TG/DTG/DSC analysis thermogram of *Cola anomala* nut shells powder

According to the TG, the *Cola anomala* nut shell powder is subdivided into four stages according to the well-defined thermal decompositions: the first mass loss at 6.54 % at 77 °C could be due to the desorption of water, the second loss of mass at 16.78 % at 219 °C could be the thermal decomposition of hemicellulose, then the third loss of maximum mass at 43.26 % at 313 °C could be the degradation of celluloses and finally the last loss of mass at 26.38 % around 440 °C could be the thermal decomposition of lignin. Beyond that, the loss of mass is less so the precursor material is more resistant to these temperature levels. We can conclude that our precursor material contains hemicellulose, cellulose and lignin thus confirming the lignocellulosic structure. The same results were obtained by Tang and Bacon which showed that the thermal decomposition of the hemicellulose is between 200 and 260 °C. Furthermore, the decomposition of the cellulose is between 240 and 350 °C. and the degradation of the lignin is between 200 and 500 °C [33]. While, the DSC shows that the pyrolysis of the powder of the nut shells of *Cola anomala* is an exothermic reaction. This curve makes it possible to obtain a product having a maximum crystallization temperature at around 440 °C.

### 3.1.2. Analysis of the obtained FTIR spectra

The FTIR spectra of the powder and activated carbons prepared from the registered *Cola anomala* nut shells are shown in Figure 2 below. Show similar profiles, but appearance and disappearance of some bands. Indeed, on these spectra, are identified the following characteristic bands decrypted using the character table.

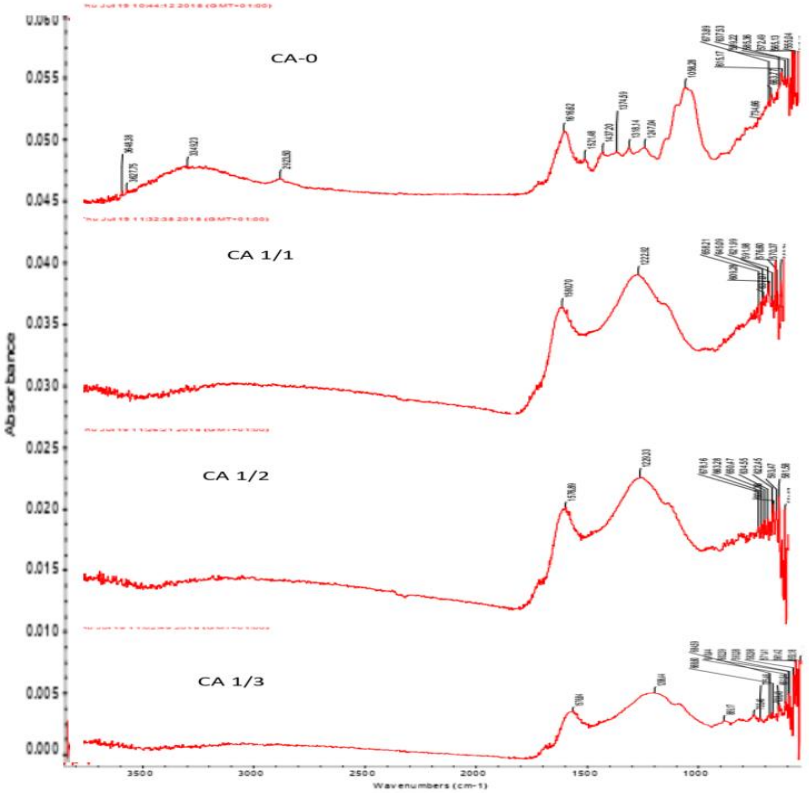


**Figure 2:** FTIR spectra of powder and activated carbons prepared from *Cola anomala* nut shells

A broad absorption band at 3648, 38 and 3627.7 $cm^{-1}$ observed on CA0 is characteristic of the hydrogen elongation vibration of hydroxyl (O-H) groups free of carboxyls, phenols or alcohols. This broad band is much lower (and almost undetectable) on the FTIR spectra of prepared activated carbons. Another broad band at 3349.23 $cm^{-1}$ is observed on CA0. It is attributed to the hydrogen elongation vibrations of the associated hydroxyl (O-H) groups of phenols or alcohols and disappears on the FTIR spectra of the impregnated and calcined powders. The FTIR spectra of CA0 shows an adsorption band at 2923.50 $cm^{-1}$ resulting mainly from the asymmetric $CH_2$ elongation vibration of aliphatic methylene. it follows a 1616.62 $cm^{-1}$ adsorption band which can be attributed to C=O elongation vibrations of ketones, aldehydes, lactones or carboxylic or C=N groups of amines.

A weak absorption band observed at 1521.48 $cm^{-1}$ on CA0 and a strong band at 1580.70 $cm^{-1}$ on CA1/1, 1576.89 $cm^{-1}$ on CA1/2 and 1576.84 $cm^{-1}$ on CA1/3 correspond to the vibrations of elongation of bonds C=C in aromatic rings. The intensity of this strong band decreases with the increase in the impregnation ratio of $H_3PO_4$.

A 1437.20 $cm^{-1}$ absorption band observed on the CA0 spectra can be attributed to both $CH_2$ deformation vibrations in the (shear) plane, asymmetric $CH_3$ shifts, and aromatic P-C elongation. Then, around 1374.04 and 1318.14 $cm^{-1}$ we have a band that can be attributed to the deformation of $CH_3$ in the symmetrical plane and to the O-H deformation of carboxyls, phenols or alcohols in the plane.

All FTIR spectra also show a low bandwidth at 1247.04 $cm^{-1}$ for CA0 and a high bandwidth at 1222.29 $cm^{-1}$ for CA1/1, 1229.33 $cm^{-1}$ for CA1/2 and 1206.44 $cm^{-1}$ for CA1/3. These bands are commonly described by the oxidized carbons corresponding to the elongation of C-O in the acid groups, alcohols, phenols, ethers and esters, but also to the elongation P-O of phosphorus and phosphocarbon compounds present in the active carbons activated by phosphoric acid. Thus CA0 shows an intense broadband at 1058.28 $cm^{-1}$ attributed to the asymmetric elongation of C-O-C.

The FTIR spectra of CA0 and CA1/3 show the absorption bands at 889.17, 775.48 and 725.46 $cm^{-1}$ for the CA1/3 and 734.66 $cm^{-1}$ for CA0 they are due to the mode of deformation out of the plane of C-H in differently substituted aromatic rings.

All the FTIR spectra also show a range of absorption band ranging from 673.89 to 547.40 $cm^{-1}$ for CA0, from 658.21 to 553.73 $cm^{-1}$ for CA1/1, 678.16 to 554.67 $cm^{-1}$ for CA1/2 and 684.59 to 544.99 $cm^{-1}$ for CA1/3. These bands are commonly described by the halogenated derivatives C- X attributed to the elongation vibrations $C-Cl$ and $C-Br$.

The presence of hydroxyl groups, carbonyls and aromatic compounds is a proof that the CA0 structure could be lignocellulosic thus confirming the observations obtained at TG. These results are consistent with those of the preparation and characterization of activated carbon from coconut and grape seeds respectively by chemical activation with phosphoric acid [34].

### 3.1.3. pH at zero charge point ($pH_{PCN}$)

The pH at zero charge point ($pH_{PCN}$) is a very important parameter that indicates the acid-base behavior of solids. In sorption studies, it is a useful parameter that makes it possible to hypothesize the ionization of functional groups on the surface of activated carbon and their interactions with adsorbates. At $pH_{PCN}$, the charge of the positive surface sites is equal to that of the negative surface sites [35].

The $pH_{PCN}$ values at zero point of loading are shown in figure 3 curve final
pH = f(initial pH).

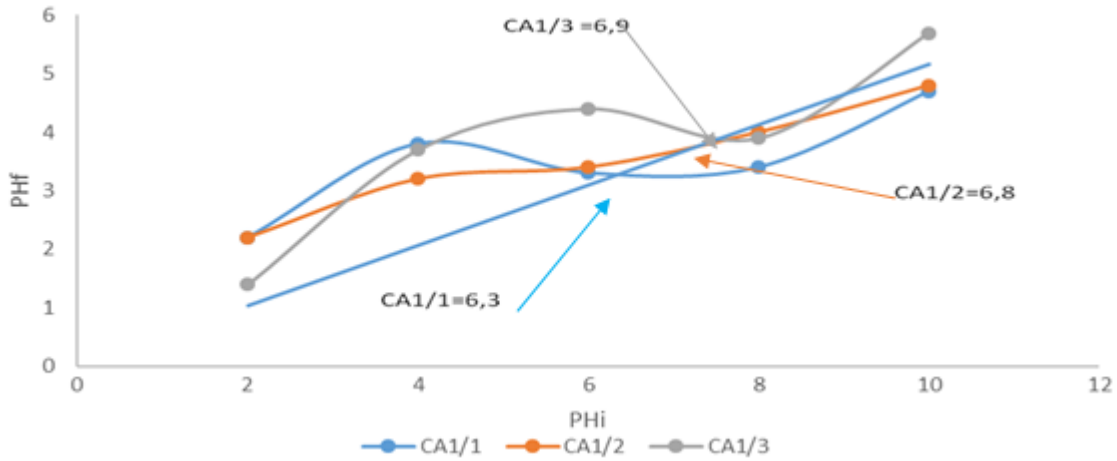


**Figure 3**: Curves representing the $pH_{PCN}$ of prepared activated carbons from *Cola anomala* nut shells

It can be seen from Figure 3 that, if the initial pH of the solution is lower than the AC $pH_{PCN}$, the surface of the AC will be positively charged, the latter will consume protons from the solution that will become less acidic. On the contrary, the surface of the AC will be negatively charged, the AC will give up its protons to the solution that will become more acidic [36].

The $pH_{PCN}$ value for CA1/2 and CA1/3 (6.8 and 6.9) respectively indicates a near neutrality of the AC. Whereas

the value 6.3 for CA1/1 indicates an acidic character of the AC. The CA1/1 result is similar to the values ($pH_{PCN}$ = 6.32, 6.19 and 6.27) reported for the preparation and characterization of activated carbon from cocoa pods by chemical activation with zinc chloride. and iron chloride, respectively [37].

### 3.1.4. Iodine and methylene blue number, specific surface and ash rate of the AC

**Table 1:** Values of iodine number, MB, $S_{I2}$, $S_{MB}$ and ash rate

| Activated carbon | CA1/1 | CA1/2 | CA1/3 |
|---|---|---|---|
| Iodine number $I_2$ ( mg/g) | 431.46 | 634.50 | 685.26 |
| Surface $S_{I2}$ ($m^2/g$) | 436.19 | 641.45 | 692.77 |
| MB number (mg/g) | 24.82 | 24.94 | 24.98 |
| Surface $S_{BM}$ ($m^2/g$) | 81.79 | 82.18 | 82.32 |
| MB rate (%) | 99.29 | 99.76 | 99.92 |
| Ash rate (%) | 2.00 | 2.00 | 2.00 |

It can be seen from Table 1 that the increase in the impregnation mass ratio substantially increases the development of micropores and mesopores, thereby increasing the adsorption capacity of activated carbons and thus the number of iodine and methylene blue, respectively. Indeed, active carbons that have a high iodine value have a small molecule adsorption capacity such as those responsible for tastes and odors [38]. Commercial activated carbons have an iodine value between 500-1500 $m^2/g$ [39]. So, CA1/2 and CA1/3 are the best prepared adsorbents. In addition, the increase in the specific surface area by adsorption of iodine and methylene blue is justified by a development of the AC porosity.

The ash rate obtained are relatively very low of about 2% for all the activated carbons prepared. The low rate of ash implies that biomass consists essentially of organic matter, and therefore of the majority carbon element. This parameter has a significant effect on the quality of AC. As a result, more than a high ash content decreases the specific surface area. Because the pores of the carbon structure are clogged by inorganic ash materials that make the activation process difficult [40]. The almost similar values ($I_2$, 656.945, 513.945 and 441.612 mg/g), (MB, 90%) and (C%, 5.47) were reported from the preparation and characterization work of the activated carbons from the shells nut *Cola accuminata* by chemical activation [41]. The values obtained in this part are an omen of good quality on activated carbons that we have prepared.

### 3.2. Adsorption study in batch mode

#### 3.2.1. Influence of contact time

The evolution of the adsorbed adsorption capacity of the EBT during the experimentation time is presented in the following figure 4.

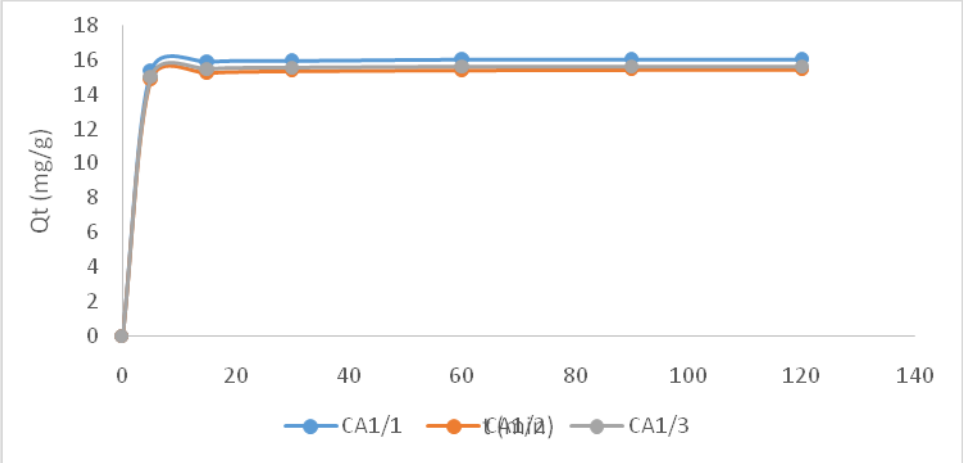


**Figure 4:** Influence of contact time on the adsorption capacity of EBT on the three activated carbons, conditions (m = 0.1 g, Ci = 60 mg / l, V = 30 ml, ambient temperature T(25±2 °C))

We note that Figure 4 presents two distinct phases: rapid adsorption at the beginning and then saturation spreading. The first phase shows that a rapid increase in the adsorption capacity of EBT takes place in few minutes (20 minutes) for all three activated carbons, this increase being due to the number of vacant sites available on the surface of the activated carbon. [42]. Thus, a second, slower phase which can last from 20 to 120 minutes in which the adsorption capacity increases slightly until reaching a landing which reflects the final equilibrium state, due to the fact that the intra-particle diffusion tends to cancel, that is, all adsorption sites become occupied in the presence of high EBT content [43]. We consider that the adsorption of EBT on the activated carbon is a fast process, since a close equilibrium time of 20 minutes is obtained. Beyond the adsorbed amount remains substantially constant up to 120 minutes of reaction. Generally, all these results revealed that the equilibrium is established after approximately 60 minutes for CA1/1 and CA1/3 and 90 minutes for CA1/2.

#### 3.2.2. Influence of initial concentration

The results obtained are shown in figure 5 below.

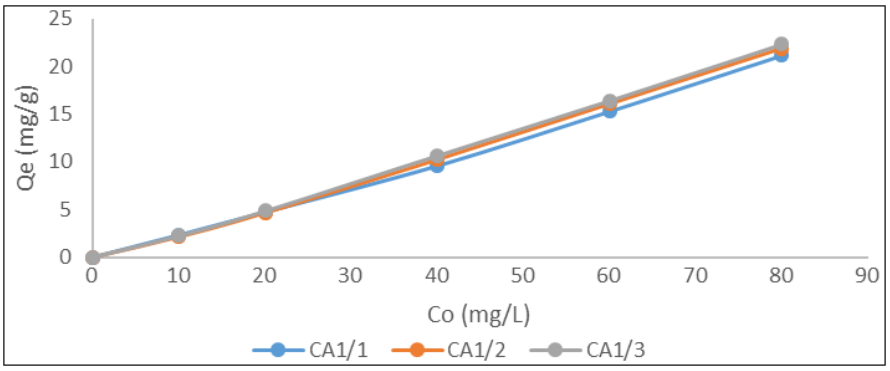


**Figure 5:** Adsorption capacity of the EBT as a function of the initial concentration EBT, conditions (m = 0.1 g, contact time t = 120 min, V = 30 ml, room temperature T (25±2 °C))

We noticed that the amount of adsorbate fixed on the activated carbon increases with the increase of the solution content in Eriochrome Black T without reaching the adsorption equilibrium for all the three AC used. This is justified by the non-saturation of the active sites on the surface in the presence of the EBT. In fact, the increase in concentration induces the elevation of the driving force of the concentration gradient, thus increasing the diffusion of the dye molecules in solution through the surface of the adsorbent [44].

### 3.3 Kinetic models

The experimental results are shown in the following figure 6 and the parameters of all three kinetic models used including the correlation coefficient $R^2$ are compiled in the following Table 2.

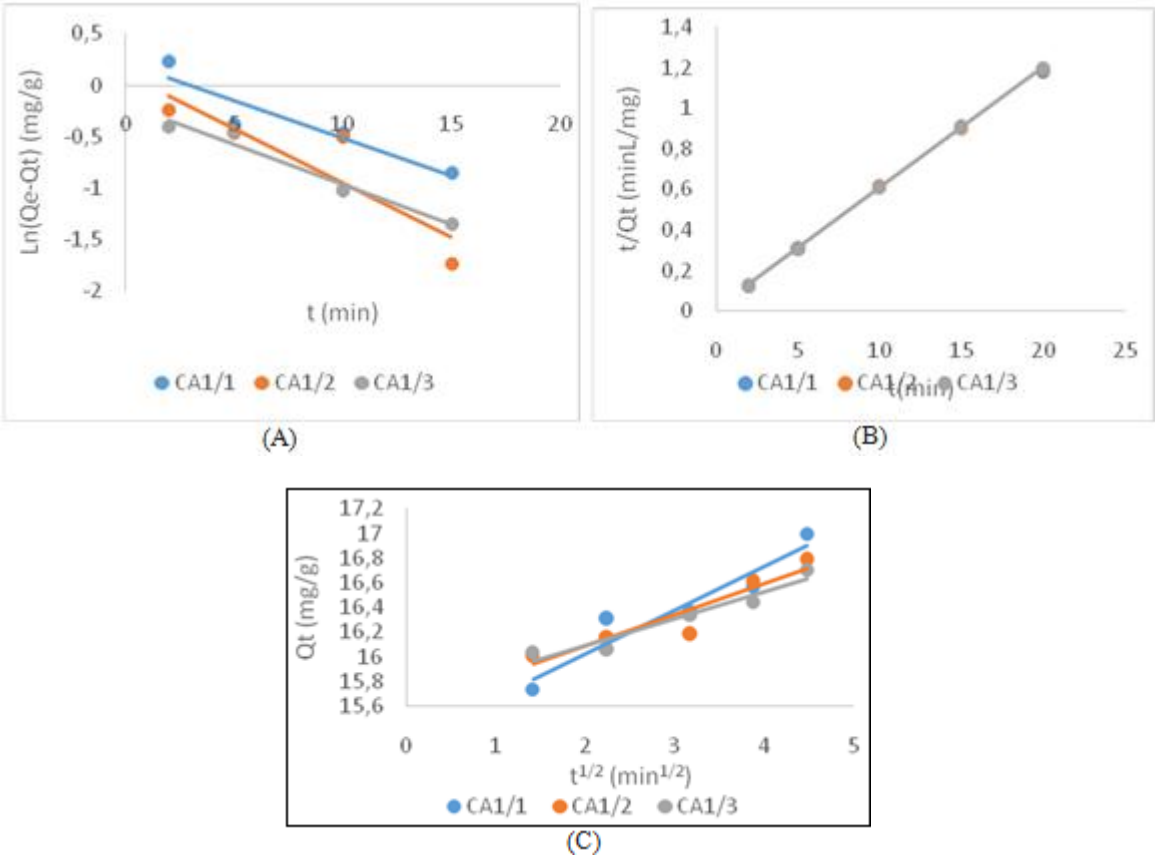


**Figure 6**: Kinetic model of the pseudo (first (A) and second (B) order) and intra-particle diffusion (C) of EBT adsorption on AC conditions (m = 0.1 g, $C_i$ = 60 mg / L, V = 30 ml, room temperature T(25±2 °C))

**Table 2:** Constants of kinetic adsorption models of EBT on AC and R²

| *Models* | *Parameters* | *CA1/1* | *CA1/2* | *CA1/3* |
|---|---|---|---|---|
| Pseudo-first order | $R^2$ | 0.8574 | 0.7895 | 0.9620 |
| | $K_1$ ($min^{-1}$) | 0.0723 | 0.1049 | 0.0782 |
| | $\Delta q$ | 15.7572 | 15.6843 | 15.8659 |
| | $Q_e$(th) (mg/g) | 1.2359 | 1.1070 | 0.8327 |
| | $Q_{emax}$ (exp) | 16.9930 | 16.7916 | 16.6983 |
| | $t_{1/2}$ (min) | 9.5850 | 6.6063 | 8.8619 |
| Pseudo-second order | $R^2$ | 0.9995 | 0.9997 | 0.9998 |
| | $K_2$ (g/mg.min) | 0.2173 | 0.2577 | 0.3269 |
| | $Q_e$ (th) (mg/g) | 17.0648 | 16.8919 | 16.7504 |
| | $Q_{emax}$ (exp) (mg/g) | 16.9930 | 16.7916 | 16.6909 |
| | $\Delta q$ | 0.0718 | 0.1003 | 0.0595 |
| | h (mg/g.min) | 63.2910 | 73.5312 | 91.7203 |
| | $t^{1/2}$ ($min^{-1}$) | 0.2696 | 0.2297 | 0.1826 |
| Intra-particule diffusion | $R^2$ | 0.9063 | 0.8822 | 0.9337 |
| | $K_{id}$ (mg/g.$min^{1/2}$) | 0.3528 | 0.2539 | 0.2169 |
| | I (mg/g) | 15.3240 | 15.5840 | 15.6570 |

It appears from fig. 6. A that all lines are non-linear and Table 2 gives satisfactory values of correlation coefficients ($R^2 \leq 0.9620$) but a large relative difference indicates non-compliance of experimental and theoretical values; the kinetic rate constant is low and the half-adsorption time is large. So the pseudo-first-order model does not better describe the elimination of EBT over AC.

As for the pseudo-second-order model, the results obtained show a perfect linearity of the regression lines of our prepared active carbons, the correlation coefficients are much better ($R^2 \geq 0.9995$) very close to unity, the different differences are small (the $Q_e$ calculated from the kinetic equation 2nd order are consistent with those obtained experimentally), the kinetic rate constant increases with the impregnation ratio of phosphoric acid as well as, the initial speed of adsorption, thereby confirming that the specific surface increases with the mass ratio but, in contrast with the half-adsorption time (Fig. 6 B and Table 2). In view of the foregoing we can conclude that the pseudo-second-order model better describes the adsorption of EBT on activated carbons prepared from the sehlls of *Cola anomala* nuts.

Regarding the intra-particle scattering model, Fig. 6 C. above clearly shows that not all straight lines are traced by the origin, the values of I different from zero, with the correlation coefficients $R^2 \leq 0.9337$, these indicate that the diffusion in the pores is involved in the sorption process but is not the only limiting mechanism of adsorption kinetics and it seems that the extra-particulate diffusion mechanism is also involved. In addition, the effect due to the diffusion boundary layer increases with the rate of the biomass impregnating agent (CA1/1, C1/2, CA1/3), respectively. The higher I is, the greater the effect of the boundary layer is important.

### 3.4 Isothermal models

The experimental results are shown in the following figure 7 and the parameters of all the two models of isotherms used including the correlation coefficient R² are grouped in the following Table 3.

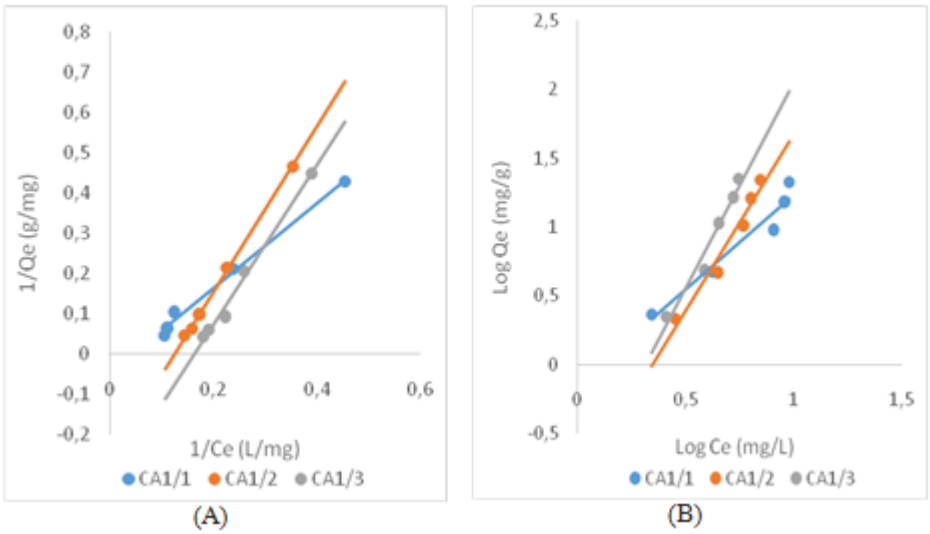


**Figure 7:** EBT adsorption isotherms on AC according to Langmuir (A) and Freundlich (B) conditions (m = 0.1 g, contact time t = 120 min, V = 30 ml, room temperature T(25±2 °C))

**Table 3:** Parameters of adsorption isotherms of EBT on CA and $R^2$

| Models | Parameters | CA1/1 | C1/2 | CA1/3 |
|---|---|---|---|---|
| Langmuir | $R^2$ | 0.9920 | 0.9990 | 0 .9916 |
| | $Q_{max}$ (mg/g) | - | - | - |
| | $K_L$ ($L.mg^{-1}$) | - | - | - |
| | $R_L$ | - | - | - |
| Freundlich | $R^2$ | 0.9440 | 0.9647 | 0.9623 |
| | $K_f$ ($mg^{1-(\frac{1}{n})}.L^{1/n}.g^{-1}$) | 0.6700 | 0.1300 | 0.1200 |
| | $n_f$ | 0.7200 | 0.3900 | 0.3300 |
| | $1/n_f$ | 1.3900 | 2.5680 | 2.9892 |

In the light of these results, the Langmuir isotherm shows that the maximum amount of adsorbed EBT $Q_{max}$ could not be determined because the intercept is negative. This could be due to the weight of the isothermal points corresponding to the very low concentrations of EBT. In this case, the determination of $Q_{max}$ is not possible because the adsorption capacity $Q_{max}$ could not take the negative values. Similarly, the parameter $K_L$ could not be determined because it is deduced using $Q_{max}$. Same for $R_L$ [45].

According to the Freundlich model, the parameter 1 / $n_f$ is greater than 1, indicates that the adsorption of the EBT on the CAs is unfavorable because the adsorption bonds become weak and the adsorption capacity decreases. Similarly, $n_f < 1$, proves that the adsorption is unfavorable. It should also be noted that $K_f$ is low, which implies that the adsorbent has a low adsorption capacity of the EBT.

The values of the regression coefficients indicate that the EBT adsorption process on activated carbon is better described by the Freundlich model with $R^2 \geq 0.94400$, while the negative constants of the Langmuir model imply the inadequacy of this one for the adsorption of EBT on AC. Recall that the Freundlich model, of an empirical nature, is used to describe it heterogeneous adsorption whereas the Langmuir model suggests that the adsorption of the molecules takes place on a homogeneous surface in monolayer without interaction between the adsorbed molecules [46 ].

### 3.5 Influence of temperature and thermodynamic parameters

Parameters such as variation of free energy (ΔG°), free enthalpy (ΔH°) and entropy (ΔS°) were determined from the experimental results obtained at different temperatures (30, 35, 40, 50 and 60 ° C) using the following equations:

$$\Delta G° = \Delta H° - T\Delta S° \quad (17)$$

Where: ΔG° is the variation of free energy (kJ.mol$^{-1}$), R is the constant of perfect gases (8.314 J. mol$^{-1}$, K$^{-1}$), T is the absolute temperature (K).

$$K_d = \frac{Q_e}{C_e} \quad (18)$$

Where: $K_d$ is the distribution coefficient, $Q_e$ is the amount of EBT absorbed at equilibrium and It is the concentration of EBT at equilibrium.

The values of ΔH° and ΔS° can be calculated from the Van't Hoff equation as follows:

$$\text{Ln } K_d = -\frac{\Delta H°}{RT} + \frac{\Delta S°}{R} \quad (19)$$

The experimental results allowed us to draw Figure 8 (A and B)

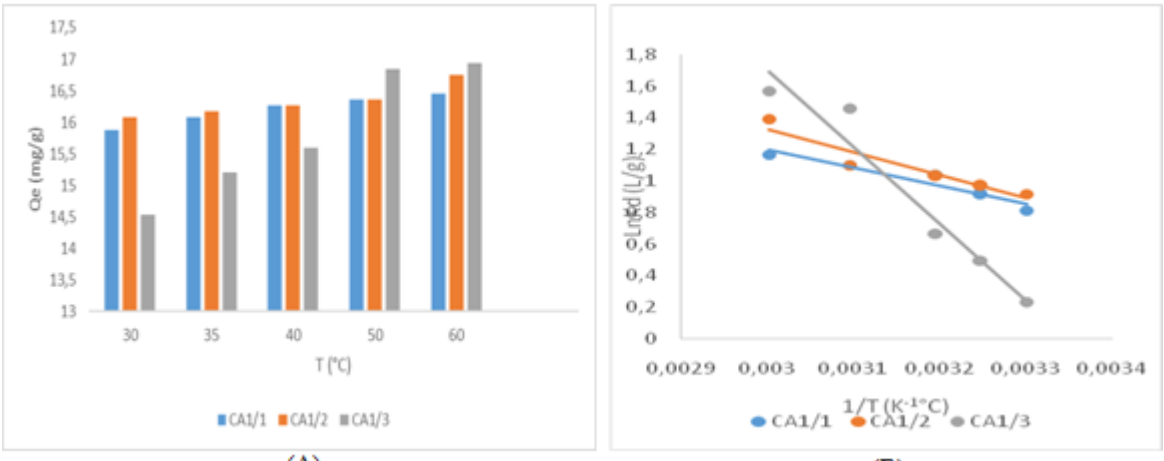


(A) (B)

**Figure 8:** Influence of the adsorption temperature of the EBT on AC (A) and representation of Ln ($K_d$) as a function of (1 / T) (B) conditions (m = 0.1 g, contact time t = 30 min, $C_i$ = 60 mg/L, V = 30 mL, pH = 3.1)

Figure 8.A shows an increase in EBT retention on activated carbon as a function of temperature increase, indicating that the reaction is endothermic. The rise in temperature favors a small increase in the adsorbed amount of EBT. So, the best results are obtained in the high temperature range. The thermodynamic parameters and the correlation coefficient $R^2$ are grouped in the following Table 4.

**Table 4:** Thermodynamic parameters relating to the adsorption of EBT on CA and $R^2$

| AC | Temperature (°K) | $\Delta G°$ $(KJ/mol)$ | $\Delta H°$ (KJ/mol) | $\Delta S°(J.mol^{-1}.K^{-1})$ | $R^2$ |
|---|---|---|---|---|---|
| CA1/1 | 303.0000 | -4.9600 | 21.8400 | 88.4500 | 0.9185 |
| | 308.0000 | -5.4000 | | | |
| | 313.0000 | -5.8400 | | | |
| | 323.0000 | -6.7400 | | | |
| | 333.0000 | -7.6100 | | | |
| CA1/2 | 303.0000 | -5.1600 | 28.0700 | 109.6800 | 0.9016 |
| | 308.0000 | -5.7100 | | | |
| | 313.0000 | -6.2600 | | | |
| | 323.0000 | -7.3600 | | | |
| | 333.0000 | -8.4500 | | | |
| CA1/3 | 303.0000 | -1.3900 | 93.9700 | 314.6800 | 0.9447 |
| | 308.0000 | -2.9500 | | | |
| | 313.0000 | -4.5200 | | | |
| | 323.0000 | -7.6700 | | | |
| | 333.0000 | -10.8200 | | | |

From these results, we observed that the negative values of free energy $(\Delta G°)$ in all AC indicate the feasibility of the adsorption process and its spontaneous nature. Besides, the adsorption process of EBT over AC is dominated by physisorption (governed by weak interactions) because, free energy values are low and below 20 KJ/mol regardless of temperature [45,47]. So, the increase in $(\Delta G°)$ with the Temperature increase shows that adsorption is more favorable at high temperature. Positive free enthalpy $(\Delta H°)$ values for the EBT retention process confirm the endothermic nature of the previously reported process and higher temperature facilitates adsorption. While, the positive values of entropy $(\Delta S°)$ (very disordered, different orientations of the EBT molecules in the surface of the AC) reflect the good affinity of the EBT opposite the AC and indicates the randomness at the solid / liquid interface during the adsorption of EBT on the different AC used [48].

## 4. Conclusion

The objective of this work is to prepare an active carbon with the best adsorption properties from the shells of *Cola* nuts (*anomala)* for the reduction of Eriochrome Black T in aqueous medium. The analysis of the TG curve shows the presence of hemicellulose, cellulose and lignin thus confirming the lignocellulosic structure. The most adsorbents of activated carbons prepared are CA1/2 and CA1/3 samples. The surface of these activated carbons is almost neutral compared to the values of the pH of point of zero charge. These have a microporosity and a mesoporosity on their surfaces. The kinetic model of the pseudo-second order better describes the adsorption of EBT on AC with $R^2 \geq 0.9995$. The thermodynamic study gave the negative values of the free energy which justify the spontaneous nature of the process and the adsorption is of physical type, the positive values of the free enthalpy which translate that the endothermic process and the positive values of the entropy that reflect EBT good affinity to AC due to pore swellings.

## References

[1] **Khoulalene, L., Semmar, S. (2016).** "Étude Cinétique et Thermodynamique de l'Adsorption du Noir Erichrome T sur le Charbon". Memoire de Master Université A. Mira-Béjaia, 89.

[2] **Dubenskaya, L. O., Levitskaya, G. D. (1999).** "Use of Eriochrome Black T for the polarographic determination of rare-earth metals". *Journal of analytical chemistry*, 54 (7), 655-657. (ISSN 1061-9348, lire en ligne).

[3] **Shabudeen, P. S. S. (2011).** "Study of the removal of malachite green from aqueous solution by using solid agricultural waste", Res.J.Chem.Sci, 1(1), 804-17.

[4] **Meunier, F., Liang-Ming Sun. (2003).** "Adsorption-Aspects théoriques, Techniques de l'Ingénieur", 27 (30).

[5] **Das Kumar, M., Attar, J.S. (2011).** "Comparative study of batch adsorption fluoride using commercial and natural adsorbent", Res.J.Chem.Sci, 1 (7), 68-75.

[6] **Muthusamy, P., Murunga, S., Manothi, S. (2012).** "Removal of Nickel ion from industrial waste water using maize cobs", ISCA.J.Biological.Sci, 1(2), 7-11.

[7] **Theivarasu, C., Mylsamy, S., Sivakumar, N. (2011).** " Adsorptive removal of crystal violet dye using agricultural waste cocoa (theobroma cocoa) shell", *Res.J.Chem.Sci*, 1(7), 38-45.

[8] **Van der Hoek, J.P., Hofman, J., Graveland, A. (1999).** " The use of biological activated carbon filtration for the removal of natural organic matter and organic micropollutants from water", *Water Sci. and Technol*., 40 (9), 257-264.

[9] **Sircar, S., Golden, T. C., Rao B. (1996, 2007).** "Activated carbon for gas separation and storage", *carbon*, 34 (1), 1-12. *Wrench J., Origin, J. of the American Oil Chemists'Society,* 8(12), 441-453.

[10] **Thibault-Starzyk F. (2004).** Les Matériaux Micro et Mésoporeux Caractérisation, EDP Sciences, 303.

[11] **Guo, Y., Rockstraw, D. A. (2007**). " Physicochemical properties of carbons prepared from pecan shell by phosphoric acid activation". *Bioresource Technology*, **98** (8), 1513-1521.

[12] **Martínez de Yuso, A., Rubio, B., Teresa Izquierdo, M. (2014).** " Influence of activation atmosphere used in the chemical activation of almond shell on the characteristics and adsorption performance of activated carbons". *Fuel Processing Technology*., 119, 74-80.

[13] **Sartape, A., Mandhare, A., Salvi, P., Pawar, D., Raut, P., Anuse, M., Kolekar, S. (2012).** " Removal of Bi (III) with Adsorption Technique Using Coconut

Shell Activated Carbon". *Chinese Journal of Chemical Engineering*, **20** (4), 768-775.

[14] **Cazetta, LA., Junior, PO., Vargas, MMA., Da silva, PA., Zou, X., Asefa, T., Almeida, CV. (2013).** "Thermal regeneration study of high surface area activated carbon obtained from coconut shell: Characterization and application ofresponse surface methodology ". *Journal of Analytical and Applied Pyrolysis.* 101, 53-60.

[15] **Girgis, BS., El-Hendawy, AA. (2002).** "Porosity development in activated carbons obtained from date pits under chemical activation with phosphoric acid. *Micropor. Mesopor* ". *Mater,* 52 (2), 105-117.

[16] **Aygün, A., Yenisoy-Karakaş, S., Duman, I. (2003).** "Production of granular activated carbon from fruit stones and nutshells and evaluation of their physical, chemical and adsorption properties". *Microporous and Mesoporous Materials*, 66 (2-3), 189-195.

[17] **Attia, AA., Girgis, BS., Fathy, NA. (2008).** "Removal of methylene blue by carbon derived from peach stones by $H_3PO_4$ activation: batch and column studies ". *Dyes Pigments*, 76 (1), 282-289.

[18] **Puziy, AM., Poddubnaya, OI., Martinez-Alonso, A., Suarez-Garcia, F., Tascon, J. MD. (2005).** "Surface chemistry of phosphoruscontaining carbons of lignocellulosic origin". *Carbon*, 43 (14), 2857-2868.

[19] **Ahmed Hared, I., Dirion, JL., Salvador, S., Lacroix, M., Rio, S. (2007**). "Pyrolysis of wood impregnated with phosphoric acid for the production of activated carbon: kinetics and porosity development studies". *J Anal Appl Pyrolysis.*, 79 (1), 101-105.

[20] **Vargas, AMM., Cazetta, AL., Garcia, CA., Moraes, JCG., Nogami, EM., Lenzi, E., Costa, WF., Almeida, VC. (2011).** "Preparation and characterization of activated carbon from a new raw lignocellulosic material: Flamboyant (*Delonix regia*) pods". *Journal of Environmental Management.*, 92 (1) 178-184.

[21] **Tsai, WT., Chang, CY., Wang, SY., Chang, CF., Chien, SF., Sun, HF. (2001)**." Preparation of activated carbon from corn cob catalyzed by potassium salts and subsequent gasification with $CO_2$". *Bioresource Technology.*, 78 (2), 203-208.

[22] **Ioannidou, O., Zabaniotou, A. (2007).** "Agricultural residues as precursors for activated carbon production—A review". *Renewable and Sustainable Energy Reviews.*, 11 (9), 1966-2005.

[23] **Romero-Anaya, AJ., Ouzzine, M., Lillo- Ródenas, MA., Linares-Solano, A. (2014**). "Spherical carbons: Synthesis, characterization and activation processes". *Carbon*, 68, 296-307.

[24] **Basta, AH., Fierro, V., El-Saied, H., Celzard, A. (2009).** "Steps KOH activation of rice straw: an efficient method for preparing high-performance activated carbons". *Bioresour. Technol*, 100 (17), 3941-3947.

[25] **Arjmand, C., Kaghazchi, T., Seyed, ML., Soleimani, M. (2006).** "Chemical Production of Activated Carbon from Nutshells and Date Stones". *Chem. Eng. Technol*, 29 (8), 986-991.

[26] **Verla, AW., Horsfall (Jnr), M., Verla, EN., Spiff, AI., Ekpete, OA. (2012**)." Preparation and Characterization of Activated Carbon from fluted PUMPKIN (*TELFAIRIA OCCIDENTALIS HOOK.F*) seed shell". *Asian Journal of Natural & Applied Sciences*, 1 (3), 39-50.

[27] **Foo, KY., Hameed, BH. (2012**). "Preparation, characterization and evaluation of adsorptive properties of orange peel based activated carbon via microwave induced $K_2CO_3$ activation". *Bioresource Technology*, 104, 679-686.

[28] **Prauchner, MJ., Rodriguez-Reinoso, F. (2008).** " Preparation of granular activated carbons for adsorption of natural gas". *Microporous Mesoporous Mater,* 109 (1-3), 581-584.

[29] **Demiral, H., Demiral, I., Karabacakoglu, B., Tümsek, F. (2011).** "Production of activated carbon from olive bagasse by physical activation". *Chemical Engineering Research and Design*, 89 (2), 206-213.

[30] **Mbaye, G. (2014). "**Développement de charbon actif à partir de biomasse lignocellulosique pour des applications dans le traitement de l'eau". Thèse de doctorat en technologie de l'Eau, de l'Energie et de l'Environnement. 2iE, Burkina Faso, 215.

[31] **Lopez-Ramon, M. V., Stoeckli, F., Moreno-Castilla, C., Carrasco-Marin, F. (1999).**"On the Characterization of acidic and basic surface sites on carbons by various techniques", *Carbon*, 37, 1215-1221.

[32] **Adamson, A.W. (1982).** *Physical chemistry of surfaces 4 ème Edition. John wiley and sons : New York.*

[33] **Tang, M.M., Roger, B. (1964).**"Pyrolysis in Organic Chemicals from Biomass", *Carbon*, 2,211-220.

[34] **Al Bahri, M., Calvo, L., Gilarranz, M. A., Rodriguez, J. J. (2012).**"Activated carbon from grape seeds upon chemical activation with phosphoric acid : Application to the adsorption of diuron from water". *Chemical Engineering Journal*, 203, 348-356.

[35] **Martínez de Yuso, A., Rubio, B., Teresa Izquierdo, M. (2014).**"Influence of activation atmosphere used in the chemical activation of almond shell on the characteristics and adsorption performance of activated carbons". *Fuel Processing Technology,* 119, 74-80.

[36] **Ndi, J., Ketcha, J., Anagho, S., Ghogomu, J., Belibi, D. (2014).**"Physical and chemical characteristics of activated carbon prepared by pyrolysis of chemically treated cola nut (*Cola accuminata*) shells wastes and its ability to adsorbs organics". *International Journal of advanced chemical Technology*, 3 (1), 1-13.

[37] **Kede, C. (2014).**"Adsorption des ions cadmium (II) et mercure (II) par l'argile et le charbon actif préparé à l'aide des cabosses de cacao". Thèse de Doctorat de l'Université de Yaoundé I, Cameroun, 185.

[38] **Ousmaila, S. M., Adamou, Z., Ibrahim D., Ibrahim, N. (2016).** *Préparation et caractérisation de charbons actifs à base de coques de noyaux de Balanites Eagyptiaca et de Zizyphus Mauritiana J. Soc. Ouest-Afr. Chim*, 21ème, 041, 59 – 67**.**

[39] **Deng, H., Li, G., Yang, H., Tang, J., Tang. J. (2010).** "Preparation of activated carbons from cotton stalk by microwave assisted KOH and K2CO3 activation," Chemical Engineering Journal, 163 (3), 373–381.

[40] **Demirbas, A. (2004).** "Effect of initial moisture content on the yields of oily products from pyrolysis of biomass". *J. of analytical and applied pyrolysis*, 2, 803-815.

[41] **Ndi, J. S. (2014).**"Textural properties and adsorption characteristics of activated carbon prepared from cola (*C. Acuminata*) nut shells : Application for the elimination of methylene blue from aqueous solution". Thèse de Doctorat Université de Yaoundé I, Cameroun, 200.

[42] **Ousmaila, S. M., Adamou, Z., Ibrahim D., Ibrahim, N. (2016).** *Préparation et caractérisation de charbons actifs à base de coques de noyaux de Balanites Eagyptiaca et de Zizyphus Mauritiana J. Soc. Ouest-Afr. Chim*, 21ème**,** 041, 59 – 67**.**

[43] **Khoulalene, L., Semmar, S. (2016).** "Étude Cinétique et Thermodynamique de l'Adsorption du Noir Erichrome T sur le Charbon". Memoire de Master Université A. Mira-Béjaia, 89.

[44] **Kara Gozo Glu, B., Tasdemir, M., Demirbas, E., Kobya, M. (2007).** "The adsorption of basic dye (astrazon Lue FGrL) from aqueous solutions onto sepiolite, fly ash and apricot shell activated carbon: Kinetic and equilibrium studies". *J. Hazard. Mater*., 147, 297-306.

[45] **Lei Yu, Yong-ming, luo. (2014).**"The adsorption mechanism of anionic and cationic dyes by Jerusalem artichoke stalk-based mesoporous activated carbon". *J. Environ. Chem*. Eng, 2, 220-229.

[46] **Hameed, B. H., Ahmad, A. L., Latiff, K. N. A. (2007).** "Adsorption of basic dye (methylene blue) onto activated carbon prepared from rattan sawdust". *Dyes Pigm*, 75, 143-149.

[47] **Kushwaha, A. K., Gupta, N., Chattopadhyaya, M. C. (2011).**"Removal of cationic methylene blue and malachite green dyes from aqueous solution by waste materials of Daucuscarota", *Journal of Saudi Chemical Society xxx, xxx-xxx*.

[48] **Fytianos, K., Voudrias, E., Kokkalis, E. (2000).**"Sorption–desorption behavior of 2,4-dichlorophenol by marine sediments", *Chemosphere*, 40, 3–6.